

Parameter Estimation for Soil Hydraulic Properties Using Zero-Offset Borehole Radar: Analytical Method

Dale F. Rucker* and Ty P. A. Ferré

ABSTRACT

Inverse methods to obtain soil hydraulic parameters are becoming increasingly popular, due to their more rapid, complete, and robust estimations of hydraulic parameters compared with traditional direct methods. We present a method to infer hydraulic parameters based on first arrival travel time measurements made with zero-offset borehole ground penetrating radar (BGPR). Borehole ground penetrating radar offers many advantages for field-scale monitoring of transient processes including the ability to measure rapidly, over relatively large soil volumes, with high temporal resolution and to great depths. The BGPR measurements are used to infer the position of the wetting front during infiltration. The analysis makes use of critical refraction at the edge of the wetting front, which gives rise to a linear increase in BGPR travel time with time as the wetting front passes beneath the antennae. The slope of this response is used directly to calculate the hydraulic conductivity. We demonstrate that unique determination of the van Genuchten α and n parameter is not possible with BGPR data alone; at least one pressure head measurement in the dry range (early time) is required. We employ a nonlinear least squares parameter estimation code to obtain the optimal α and n parameters for synthetic data. The method could potentially be applied to areas of artificial recharge in an infiltration basin, natural recharge in an ephemeral stream, or agricultural settings where the surface is flooded with irrigated water.

SOIL HYDRAULIC FUNCTIONS, such as those that describe the unsaturated hydraulic conductivity, soil-water retention, and soil-water diffusivity as functions of pressure head, partially govern the movement of water in an unsaturated soil during absorption, infiltration, and drainage. Modeling of a wetting front during infiltration, for example, requires knowledge of these parameters to solve the Richards' equation (Richards, 1931) of unsaturated water flow in porous media. With traditional direct laboratory methods, the parameters are time-consuming to measure and require restrictive initial and boundary conditions (Hopmans and Simunek, 1999; Lambot et al., 2002). Several researchers have presented improved methods to infer soil hydraulic properties through inverse procedures, for example, Warrick (1993) and Inoue et al. (1998). We adopt the method of Warrick (1993) in which the forward model uses the simplified analytical representation of water flow given in Warrick et al. (1985). Warrick (1993) discusses how measurements of the wetting front position with time made in the laboratory, together with an assumed van Genuchten n can be used to deduce the saturated hydraulic conductiv-

ity and the van Genuchten α . In this study, we apply this approach to measurements of wetting front advance made under simulated field conditions.

Standard methods typically determine the hydraulic parameters for small disturbed soil samples. It can be difficult to make quantitative use of these measurements to characterize flow and transport in a heterogeneous field site (Wang et al., 2003). Existing field methods are intrusive and/or disruptive of the flow system under study (Inoue et al., 1998) and are often limited to near surface measurement (Perroux and White, 1988). It would be advantageous to infer the hydraulic properties at the field scale with a method that causes minimal disturbance to the medium in which the measurements are made. Ideally, this method would allow for profiling and mapping of the hydraulic properties.

Many geophysical methods are nonintrusive (measurements made at the ground surface) or minimally intrusive (measurements made within a borehole). As a result, these methods are good candidates for obtaining the measurements needed to infer hydraulic properties (e.g., Binley et al., 2002; Hubbard et al., 1998; Yeh et al., 2002). In addition, many of these methods are rapid and measure over scales of interest that are more representative for field scale characterization of vadose zone processes. Finally, borehole methods can offer high resolution profiling of hydrologic properties to great depths, which may lead to the ability to profile soil hydraulic properties. High frequency electromagnetic techniques, such as ground penetrating radar (GPR) and time domain reflectometry (TDR), provide robust indirect measurements of the volumetric water content within their sample volume through the empirical correlations with the dielectric permittivity (e.g., Topp et al., 1980). Low frequency or direct current electrical methods can also provide information regarding the volumetric water content through correlation with the electrical conductivity (Archie, 1942). However, this correlation is less unique than the correlation between dielectric permittivity and volumetric water content, because electric conductivity also depends on tortuosity, electrical conductivity of the soil matrix and electrical conductivity of the pore water (de Lima and Niwas, 2000).

Rucker and Ferré (2004b) demonstrated that BGPR in zero-offset profiling (ZOP) mode could be used to monitor the advance of a wetting front. They showed that when critical refraction of the electromagnetic waves is considered, the volumetric water content profile could be determined from first arrival BGPR travel times on a radargram. High temporal and spatial resolu-

D.F. Rucker and T.P.A. Ferré, Dep. of Hydrology and Water Resources, Univ. of Arizona, Harshbarger Bldg. 11, P.O. Box 210011, Tucson, AZ 85721. Received 17 Oct. 2003. *Corresponding author (druck@hwr.arizona.edu).

Published in Soil Sci. Soc. Am. J. 68:1560–1567 (2004).
© Soil Science Society of America
677 S. Segoe Rd., Madison, WI 53711 USA

Abbreviations: BGPR, borehole ground penetrating radar; bgs, below ground surface; EM, electromagnetic; TDR, time domain reflectometry; WCAC, Western Campus Agricultural Center; ZOP, zero-off-set profiling.

tion volumetric water content profiles can then be used to infer the position of the wetting front through time. The objective of this study was to evaluate the use of ZOP BGPR first arrival travel time data in an inversion procedure to obtain the hydraulic properties that describe the van Genuchten soil-water retention and unsaturated hydraulic conductivity functions. The analysis follows the method presented in Example 2 of Warrick (1993) and is modified through the use of a nonlinear least squares parameter estimation procedure. Additionally, we set out to improve the uniqueness of the simultaneous inversion of multiple parameters through the use of minimal supporting pressure head data.

THEORY

Flow Model

The one-dimensional vertical flow of water in a homogeneous unsaturated soil is governed by:

$$\frac{\partial \theta(z,t)}{\partial t} = \frac{\partial}{\partial z} \left[D(\theta) \frac{\partial \theta(z,t)}{\partial z} \right] - \frac{\partial K(\theta)}{\partial z} \quad [1]$$

where θ is the volumetric water content ($\text{cm}^3 \text{cm}^{-3}$), D is soil-water diffusivity ($\text{cm}^2 \text{s}^{-1}$), and K is water content dependent hydraulic conductivity (cm s^{-1}). Equation [1] is referred to as the θ -based Richards' equation (Warrick, 2003) and is nonlinear because both D and K are functions of the water content. For infiltration into a soil of initially uniform volumetric water content, the following boundary and initial conditions can be assumed:

$$t = 0, z > 0, \theta = \theta_0, \quad [2a]$$

$$t \geq 0, z = 0, \theta = \theta_1, \quad [2b]$$

and

$$t \geq 0, z \rightarrow \infty, \theta = \theta_0, \quad [2c]$$

where θ_1 is the imposed volumetric water content at the top boundary when the infiltration begins and θ_0 is the background volumetric water content. Philip (1957a) developed an analytical solution to Eq. [1] and proposed that the Boltzmann transform be modified to account for gravity during vertical infiltration:

$$z(\theta,t) = \lambda t^{1/2} + \chi t + \varphi t^{3/2} + \dots \quad [3]$$

The term $z = \lambda t^{1/2}$ is the Boltzmann transform (Klute, 1952) used to solve the diffusion equation and the remaining terms in Eq. [3] are corrections for the gravity term, $\partial K(\theta)/\partial z$. The coefficients λ , χ , and φ are ordinary integrodifferential equations that are evaluated through numerical integration (Philip, 1969). Kirkham and Powers (1972) and Warrick (2003) show how to obtain all three coefficients.

Warrick et al. (1985) used the concept of similar media to scale the parameters θ , z , t , and K to dimensionless forms. A large class of hydraulic functions, including the functional forms of $K(\theta)$ and $h(\theta)$ presented by van Genuchten (1980) and Brooks and Corey (1964), can be written in dimensionless forms:

$$S_e = \frac{\theta - \theta_r}{\theta_s - \theta_r} \quad [4]$$

$$T = \frac{\alpha K_s t}{\theta_s - \theta_r} \quad [5]$$

$$Z = \alpha z \quad [6]$$

$$K^* = \frac{K}{K_s} \quad [7]$$

$$h^* = \alpha h \quad [8]$$

and

$$D^* = K^* \frac{dh^*}{dS_e} = \frac{\alpha(\theta_s - \theta_r)D}{K_s}, \quad [9]$$

where S_e is dimensionless water content (i.e., effective saturation), θ_r is the residual volumetric water content, T is dimensionless time, Z is dimensionless depth, K^* is dimensionless hydraulic conductivity, h^* is dimensionless pressure head, and α ($1/L$) is a scaling factor. Substitution of the dimensionless variables into Eq. [1] yields:

$$\frac{\partial S_e}{\partial T} = \frac{\partial}{\partial Z} \left(D^* \frac{\partial S_e}{\partial Z} \right) - \frac{\partial K^*}{\partial Z}. \quad [10]$$

The dimensionless boundary and initial conditions are:

$$S_e(Z,0) = S_{e0}, \quad [11a]$$

$$S_e(0,T) = S_{e1}, \quad [11b]$$

and

$$\lim_{Z \rightarrow \infty} S_e(Z,T) = S_{e0} \quad [11c]$$

The dimensionless series solution for Z is:

$$Z(S_{e,T}) = \lambda(S_e)T^{1/2} + \chi(S_e)T + \varphi(S_e)T^{3/2} \quad [12]$$

The series solution is valid for small times, $T < T_g$, where:

$$T_g = \frac{\left[\int_{S_{e0}}^{S_{e1}} \lambda(S_e) dS_e \right]^2}{1 - \frac{K^*(S_{e0})}{K^*(S_{e1})}}. \quad [13]$$

For late times ($T > T_g$) it has been shown that the surface intake approaches a constant value. The wetting front retains a constant shape that moves downward at an approximate rate, κ , of (Philip, 1957a; Warrick, 2003):

$$\kappa = \frac{dK}{d\theta} - \frac{d}{d\theta} \left(D \frac{d\theta}{dz} \right) \approx \frac{K(\theta_1) - K(\theta_0)}{\theta_1 - \theta_0}. \quad [14]$$

For $T > T_g$, the dimensionless solution of Eq. [12] is

$$Z(S_e, T > T_g) = Z(T_g) + \frac{(T - T_g)[K(S_{e1}) - K(S_{e0})]}{S_{e1} - S_{e0}} \quad [15]$$

Borehole Radar Travel Time Model

Borehole ground penetrating radar sends, via a transmitting antenna, unguided electromagnetic (EM) pulses from within a borehole into the surrounding subsurface (e.g., Davis and Annan, 2002). A receiving antenna in a parallel borehole records the amplitude of the pulse (in volts) as a time series. The travel time of the first arriving energy is interpreted from the time series. The travel time (τ) of the EM pulse can be related

to the dielectric permittivity of the medium, which is directly related to the volumetric water content (θ), for example:

$$\theta = a \frac{c\tau}{l} - b \quad [16]$$

where c is the speed of light, l is the distance over which the EM wave travels, and a and b are empirically derived fitting functions (Ferré et al., 1998). The term $\frac{c\tau}{l}$ is equal to the square root of the relative apparent dielectric permittivity.

In ZOP mode the transmitting and receiving antennae are located at a common depth for each measurement. It is commonly assumed that all travel times are associated with direct waves that travel along a horizontal path from the transmitter to the receiver. However, Rucker and Ferré (2003) showed that both direct and critically refracted travel paths must be considered for proper evaluation of ZOP BGPR travel time profiles. For an antennae separation distance, x , the direct travel time (τ_{direct}) is:

$$\tau_{\text{direct}} = \frac{x}{v_1} \quad [17]$$

where x is the antennae separation and v_1 is the electromagnetic propagation velocity of a moist soil. Critical refraction may occur when an EM pulse is generated in a layer of relatively low propagation velocity adjacent to a higher velocity layer. Under these conditions, the fastest travel path may be associated with energy that travels along a nonhorizontal path to the boundary, then horizontally along the boundary at a higher velocity. The critically refracted travel time of a pulse that is generated in low velocity (high water content) layer (v_1) relative to an adjacent high velocity (low water content) layer (v_0) is (Rucker and Ferré, 2003):

$$\tau_{\text{refr}} = \frac{2z}{v_1 \cos i_c} + \frac{x - 2z \tan i_c}{v_0} \quad [18]$$

where z is the vertical distance of the antennae from the boundary that divides the two layers and

$$i_c = \sin^{-1} \left(\frac{v_1}{v_0} \right) \quad [19]$$

is referred to as the critical angle. Equations [17] and [18] can be simplified by using the reciprocal of the EM propagation velocity, that is, slowness (s) (Sheriff and Geldart, 1995). Additionally, the terms $\cos(i_c)$ and $\tan(i_c)$ can be written as

$$\cos i_c = \frac{\sqrt{v_0^2 - v_1^2}}{v_0} = \frac{\sqrt{s_0^2 - s_1^2}}{\frac{1}{s_0}} \quad [20a]$$

$$\tan i_c = \frac{v_1}{\sqrt{v_0^2 - v_1^2}} = \frac{\frac{1}{s_1}}{\sqrt{\frac{1}{s_0^2} - \frac{1}{s_1^2}}} \quad [20b]$$

Substitution of the slowness and identities for the trigonometric functions, Eq. [17] and [18] can be written as (Rucker and Ferré, 2004a):

$$\tau_{\text{direct}} = s_1 x \quad [21]$$

$$\tau_{\text{refr}} = x s_1 + 2z d_s \quad [22]$$

where

$$d_s = \sqrt{s_1^2 - s_0^2} \quad [23]$$

Consider a time series of ZOP BGPR measurements made during the advance of a wetting front. The center of each antenna is located at a fixed depth for the duration of the experiment. It is also assumed that the antennae are not located near a refracting boundary before infiltration begins. That is, the first arriving travel paths before and long after infiltration are direct. Figure 1 shows a conceptualization of the infiltration experiment and associated ZOP BGPR measurements. When the position of the wetting front is above the antennae, the first arriving travel path is direct (Fig. 1A). As the wetting front moves past the antennae, the EM wave will refract critically at the edge of the front (Fig. 1B). Critical refraction will continue until the wetting front has moved past the antennae by a distance equal to the refraction termination depth (Rucker and Ferré, 2003) (Fig. 1C). Thereafter, the first arriving energy will be direct.

Parameter Estimation

To estimate the hydraulic properties from BGPR travel time measurements, the analytical water flow model is used to predict the volumetric water content profile as a function of time for a given set of hydrologic parameters. The first arriving BGPR travel time profile is then determined as a

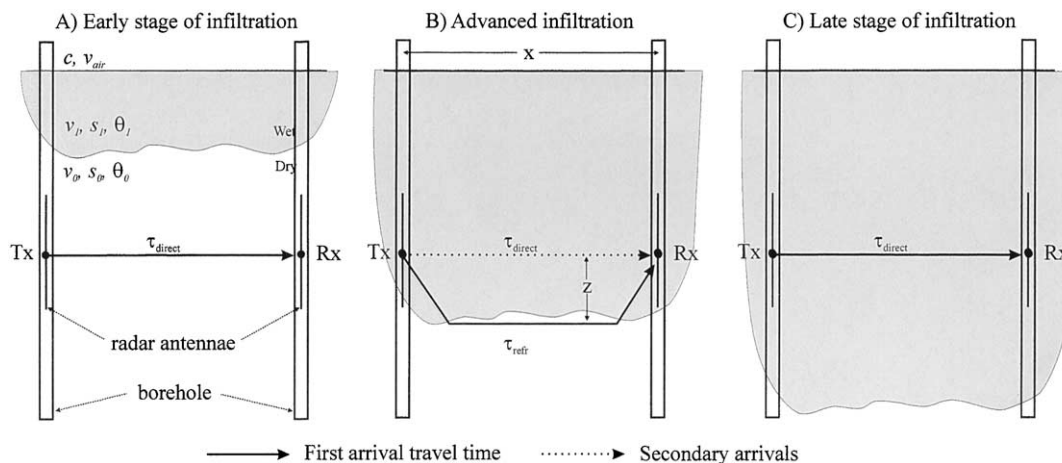


Fig. 1. Schematic representations of wetting front locations relative to zero-offset profiling (ZOP) borehole ground penetrating radar (BGPR) antennae and associated BGPR first arriving travel paths.

function of time from these volumetric water content profiles. Finally, an optimization model is used to identify the set of hydrologic parameters that minimizes the difference between the observed and simulated first arrival travel times. These differences are expressed in the following objective function, $E(\beta)$:

$$E(\beta) = \sum_{j=1}^N w_j [\tau_p(t_j) - \hat{\tau}_p(t_j, \beta)]^2, \quad [24]$$

where τ_p is the observed first arrival travel time from Path p (either direct or critically refracted) at time t_j , $\hat{\tau}_p$ is the modeled first arrival travel time from path p at time t_j subject to the soil hydraulic parameters $\beta = \{\beta_1, \beta_2, \beta_3, \dots\}$ (e.g., K_s , α , and n), and w is the weights formed by the measurement error. A free-ware parameter estimation code, PEST (Doherty, 2002), was used to find β that minimized Eq. [24] using a Levenberg–Marquardt method.

EXAMPLE

Forward Modeling of First Arriving Travel Time Profiles through Time

Equation [1] was used to determine the volumetric water content profile over a discretized time interval from 0.5 to 30 h (or in dimensionless time, $0.0309 \leq T \leq 1.8514$). The van Genuchten hydraulic functions were used to represent the soil:

$$K^*(S_e) = \sqrt{S_e} [1 - (1 - S_e^{1/m})^m]^2 \quad [25]$$

$$S_e(h^*) = (1 + |h^*|^n)^{-m}, \quad [26]$$

and

$$D^*(S_e) = \frac{1 - m}{m} S_e^{\left(\frac{1}{2} - \frac{1}{m}\right)} [(1 - S_e^{1/m})^{-m} + (1 - S_e^{1/m})^m - 2] \quad [27]$$

where

$$m = 1 - \frac{1}{n} \text{ for } 1 < n < \infty. \quad [28]$$

Hydraulic properties of $\alpha = 0.01 \text{ (cm}^{-1}\text{)}$, $K_{\text{sat}} = 0.0006 \text{ (cm s}^{-1}\text{)}$, $n = 2$, $\theta_r = 0.1 \text{ (cm}^3 \text{ cm}^{-3}\text{)}$, and $\theta_s = 0.45 \text{ (cm}^3 \text{ cm}^{-3}\text{)}$ were assigned to represent a loam soil. The background volumetric water content was $\theta_0 = 0.17 \text{ (cm}^3 \text{ cm}^{-3}\text{)}$ and the volumetric water content imposed at the surface was $\theta_1 = 0.45 \text{ (cm}^3 \text{ cm}^{-3}\text{)}$ to represent infiltration at full saturation with no ponding. Near saturation, the value for D^* was estimated following the approach of Warrick et al. (1985). For all $T < T_g$ ($T_g = 0.611$) Eq. [12] was solved for $Z(S_{e,T})$. To obtain the volumetric water content as a function of time and depth, the dependent variable was mapped to $S_e(Z, T)$ through interpolation and to $\theta(z, t)$ by transformation using Eq. [4] through [8]. Equation [15] was used for late times and the volumetric water content profile was obtained by a similar procedure as above. The modeled volumetric water content profiles through time were interpreted with a ZOP BGPR forward model (Rucker and Ferré, 2004c) to determine the first arrival travel time at 1.5 m below ground surface (bgs) as a function of time.

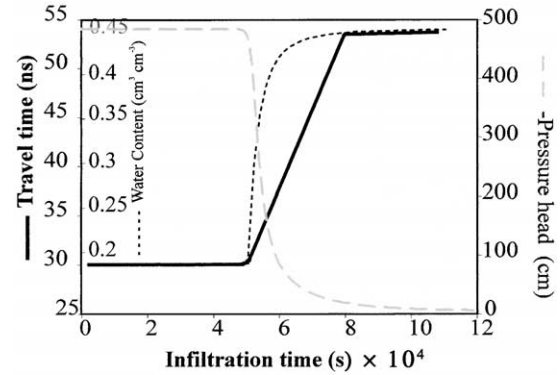


Fig. 2. Breakthrough curves of BGPR first arrival travel time, pressure head, and water content from forward modeling. Note: Infiltration time on axis to be multiplied by 1×10^4 to obtain the correct time.

Figure 2 shows the first arrival travel time during the course of the infiltration experiment and represents the measured data for subsequent inverse modeling. At early and late infiltration time, the first arrival travel time is constant. The travel times are associated with a direct wave through the medium with volumetric water contents equal to the initial volumetric water content at early time and equal to the water content behind the wetting front at late time. The middle period shows a linear increase in first arrival travel time with infiltration time. The linear increase is due to critical refraction occurring at the edge of the wetting front, which is moving downward with a constant velocity. As a comparison, Fig. 2 also includes the volumetric water content and pressure head at a point at 1.5 m bgs. These data represent measurements collected with, for example, a buried TDR probe and a tensiometer, respectively. The point measurements of volumetric water content and pressure head show initial sharp changes with time (high slope) when the wetting front first arrives at 1.5 m. The slopes then decrease as the wetting front passes the measurement depth.

In the previous examples, the soil hydraulic properties were homogeneous and the wetting front moved at a constant velocity throughout the profile. In more realistic media, where the profile may contain many layers of different hydraulic properties, the wetting front velocity can change as it passes through layers of different materials. The average velocity in a layered profile, then, will depend on the hydraulic conductivity of a particular layer (Whisler et al., 1972). As an example, consider water infiltrating into a loam soil of low hydraulic conductivity overlying a sand soil with a relatively higher hydraulic conductivity (Fig. 3A). The position of the wetting front is plotted in time; the slope of the wetting front position at any time is equal to the wetting front velocity at that time. In the loam, the velocity of the wetting front is slower than in the sand. For comparison with the layered case, the wetting front position is plotted for a homogeneous sand soil. The slopes of the wetting front positions are parallel in the sand (once the wetting front has moved away from the boundary). As a second example, a gravel of relatively large hydraulic conductivity overlies the sand soil. The speed at which

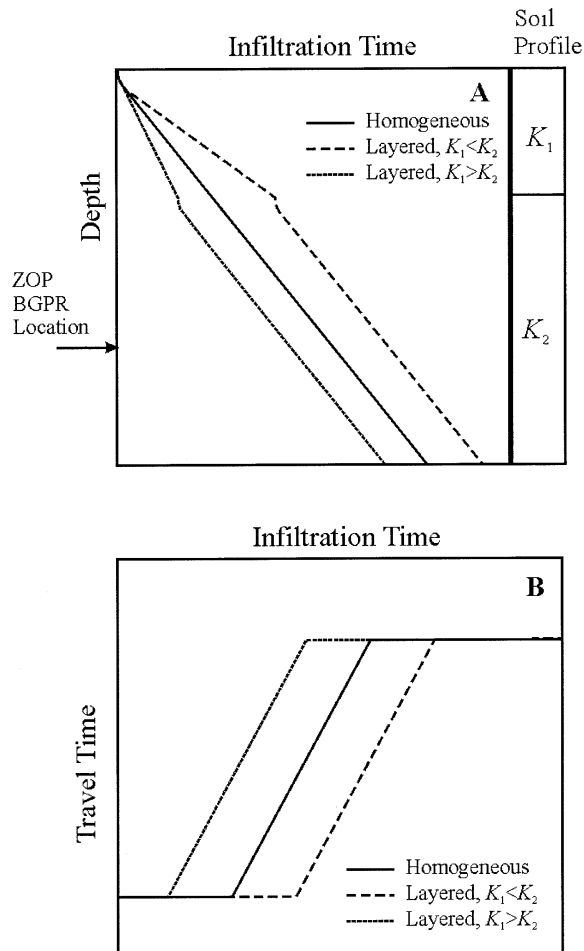


Fig. 3. Infiltration into a layered soil. (A) Wetting front position as a function of time for three cases: a homogeneous soil; $K_1 < K_2$; and $K_1 > K_2$. (B) Associated BGPR first arrival travel time curves for the three cases shown in 3A.

the wetting front moves through the gravel is greater than the sand, but is again constant in each layer. This demonstrates that while the average wetting front velocity through a layered soil is influenced by all of the media through which the wetting front has passed, the instantaneous wetting front velocity at a given depth is associated with the material properties at that depth, as long as that depth is not immediately adjacent to a boundary between soil layers.

The time series of the BGPR first arrival travel time was calculated for each of the three cases above (Fig. 3B). For the loam/sand soil combination, the arrival of the wetting front was later than in the homogeneous soil, shown as a time lag between the two first arrival travel time curves. The lag, however, does not affect on the shape of the first arrival travel time breakthrough curve.

Parameter Estimation with No Supporting Pressure Head Data

The first stage of testing of the utility of BGPR measurements for inferring hydraulic properties involved inversion of the synthetically derived first arrival travel

time profiles. The inferred hydraulic properties could then be compared with known property values. The travel times at the beginning and end of the infiltration experiment (Fig. 2), when the EM wave path were direct, were converted to volumetric water content using an empirical calibration equation (Ferré et al., 1996):

$$\theta = 0.1181 \frac{v_{\text{air}} \tau_{\text{direct}}}{x} - 0.1841 \quad [29]$$

where v_{air} is the EM velocity of propagation in air (0.3 m ns^{-1}). From the travel times shown on Fig. 2, θ_0 and θ_1 are 0.17 and $0.45 \text{ cm}^3 \text{ cm}^{-3}$, respectively. Equation [22] can be rewritten as a function of time:

$$\tau_{\text{refr}}(t) = x s_1 + 2z_f(t) d_s \quad [30]$$

where z_f is the position of the wetting front relative to the antennae and the critically refracted first arriving travel time is a function of infiltration time, t . The derivative of Eq. [30] with time yields:

$$\frac{d\tau_{\text{refr}}}{dt} = \Omega = 2d_s \frac{dz_f}{dt} \quad [31]$$

where $dz_f/dt = \kappa$ from Eq. [14]. Assuming that $K(\theta_0) = 0$, Eq. [31] can be rearranged to solve for $K(\theta_1)$:

$$K(\theta_1) = \frac{\Omega}{2d_s} (\theta_1 - \theta_0). \quad [32]$$

For infiltration at full saturation, $\theta_1 = \theta_s$ and Eq. [32] yields K_{sat} .

Using linear regression, the slope of the linear travel time increase in Fig. 2 is $0.0008 \text{ (ns s}^{-1}\text{)}$. Since the data are error free, an error analysis was not conducted on this parameter. However, if the BGPR data were obtained from field measurements, it is suggested that a proper error analysis be conducted. The slowness values at the beginning (s_0) and end (s_1) are calculated from Eq. [21] and [29] for the antennae separation of 3 m used to create the synthetic first arrival travel time profiles: $s_1 = 53.67 \text{ ns/3 m} = 17.89 \text{ (ns m}^{-1}\text{)}$ and $s_0 = 10 \text{ (ns m}^{-1}\text{)}$. The calculated K_{sat} using Eq. [32] is $0.00075 \text{ (cm s}^{-1}\text{)}$, which shows good agreement with the value used in the forward model (0.0006 cm s^{-1}). The difference between the calculated and modeled K_{sat} is due to the approximation of the wetting front velocity in Eq. [14], as shown by Philip (1957b).

To determine whether this inverse procedure can be used to determine uniquely the van Genuchten α and n parameters, we examined the error surface in α vs. n space in a manner similar to that used by Hopmans et al. (2002) (Fig. 4). That is, the first arriving travel time as a function of infiltration time was calculated for many combinations of α and n with a fixed value of K_{sat} using the forward water flow and ZOP/BGPR models. The error for each parameter combination was defined as the logarithm of the root mean square error (RMSE) between the first arrival travel time series for a base case with α and n of 0.01 cm^{-1} and 2 , and the series determined for the parameter combination:

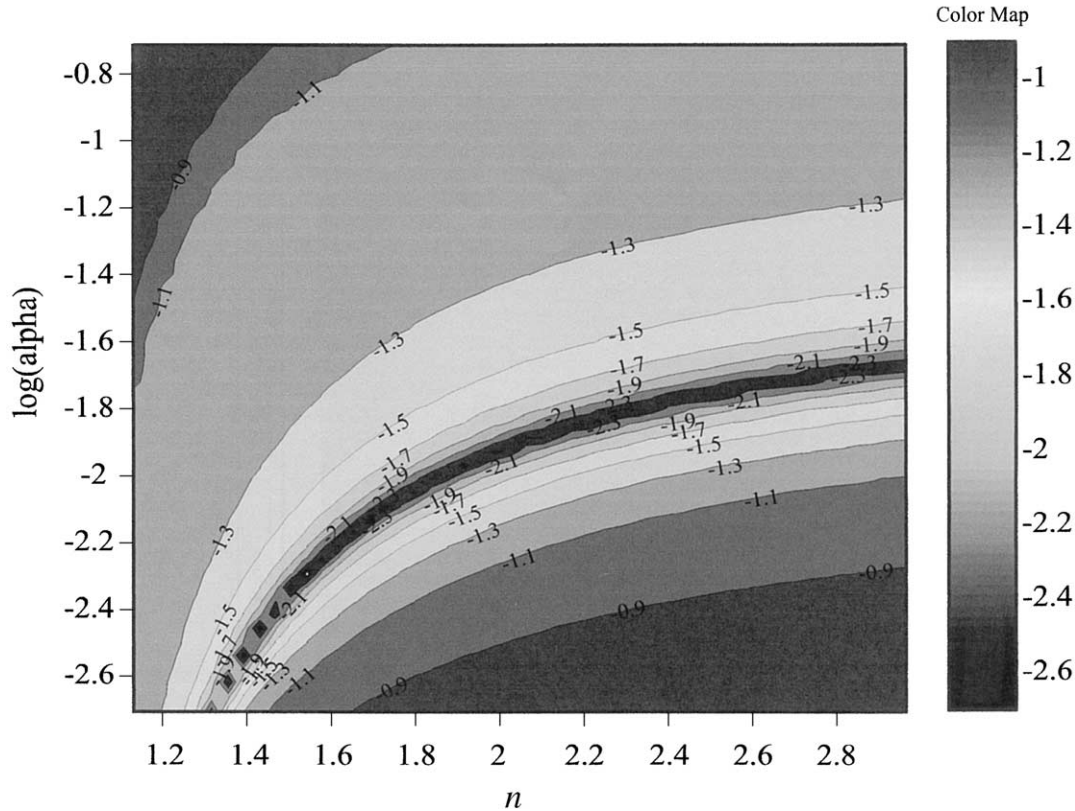


Fig. 4. Response surface from sensitivity analysis for α vs. n . The values used to form the synthetic data are $\log(\alpha) = -2$ and $n = 2$. Contoured values are the logarithm of the root mean square error between the modeled and correct first arrival travel time profiles.

$$RMSE = \sqrt{\frac{1}{N} \sum_{j=1}^N [\tau_p(t_j) - \hat{\tau}_p(t_j, \beta)]^2} \quad [33]$$

The error surface indicates that there is no unique combination of α and n that give the closest fit to a measured time series of wetting front locations. That is, the solution is non-unique based solely on wetting front travel time measurements. Specifically, there is a curved valley of minima such that there is a corresponding choice of n that will give an optimal fit for any assigned value of α (Toorman et al., 1992). This feature of the van Genuchten relationship has been shown previously (e.g., see Simunek and van Genuchten, 1996 and Vrugt et al., 2001). Warrick (1993) overcame this non-uniqueness by reducing the number of parameters to two (K_{sat} and α) by assuming that $n = 2$ and $\theta_r = 0$.

Following the approach of Warrick (1993), we assumed values of n and used PEST to determine the value of α for the results shown on Fig. 2 (Table 1).

Simulation A1, with $n = 2$ and K_{sat} determined from Eq. [32] gives an α value of 0.0077 cm^{-1} , with a 95% confidence interval of ± 0.0003 . The estimated value is slightly lower than the value used in the forward flow simulation (0.01 cm^{-1}). For Simulation A2, n was 2 and K_{sat} was decreased to $0.00065 \text{ cm s}^{-1}$; this resulted in an increase in α to $0.0136 \pm 0.0003 \text{ cm}^{-1}$, which slightly exceeds the correct value of 0.01 cm^{-1} . For simulation A3, n was set to 2.5 and the value of K_{sat} determined from Eq. [32] was used. The fitted α value ($0.0116 \pm 0.0002 \text{ cm}^{-1}$) showed the closest agreement with the known value. Despite the relatively good agreements of the α values with the known value, the retention curves determined from Simulations A1 through A3 differ significantly from the retention curve based on the properties used in the forward model (Fig. 5A). Specifically, the curves for simulation A1 and A2 have the same shape as the correct retention curve, but are offset in the dry range. The higher n value used for

Table 1. Simulation results for inverse parameter estimation.

Simulation	Measured data	Parameter	Initial α cm^{-1}	Guess n	K cm s^{-1}	Final α cm^{-1}	Estimate n	$E(\beta)$
Simulation A								
A1	τ	α	0.002	2	0.00075	$0.0077 \pm 0.0003^\dagger$	-	5.2
A2	τ	α	0.002	2	0.00065	$0.0136 \pm 0.0003^\dagger$	-	5.6
A3	τ	α	0.002	2.5	0.00075	$0.0116 \pm 0.0002^\dagger$	-	5.0
Simulation B								
B1	τ, h	α, n	0.002	1.5	0.00075	$0.0088 \pm 0.0001^\dagger$	$2.07 \pm 0.007^\dagger$	10.9
B2	τ, h	α, n	0.06	4.5	0.00075	$0.0086 \pm 0.0001^\dagger$	$2.1 \pm 0.006^\dagger$	4.5

† 95% confidence limits.

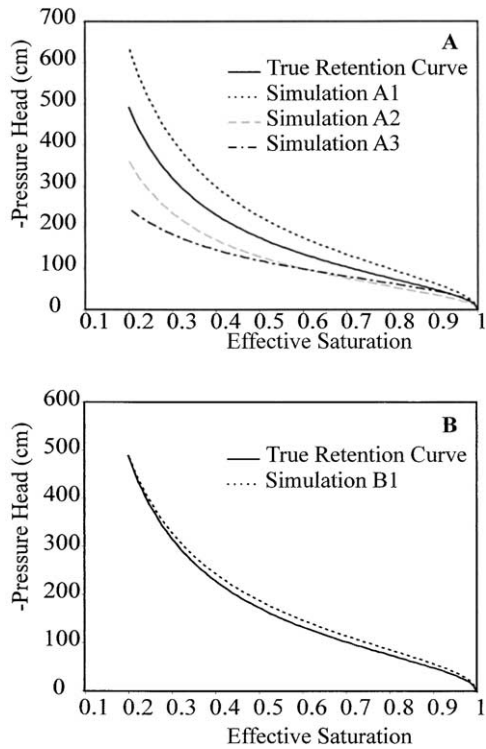


Fig. 5. Retention curves from the estimated hydraulic properties presented in Table 1.

Simulation A3 gives rise to a retention curve with a very different shape than that of the medium used in the forward simulation.

Parameter Estimation with Supporting Pressure Head Data

Several researchers have addressed the problem of finding the global minimum on a non-unique error surface for hydrologic problems with two or more unknown parameters (e.g., Finsterle and Faybishenko, 1999; Gribb, 1996; Parker et al., 1985; Si and Kachanoski, 2000). Generally, this is achieved through the addition of supporting data, for example, pressure head at a fixed location. A pressure head measurement can be added to the objective function as:

$$E(\beta) = A \sum_{j=1}^N w_j [\tau_p(t_j) - \hat{\tau}_p(t_j, \beta)]^2 + B \sum_{i=1}^M u_i [h(t_i) - \hat{h}(t_i, \beta)]^2, \quad [34]$$

where $h(t)$ is the measured pressure head, $\hat{h}(t, \beta)$ is the modeled pressure head, \mathbf{u} is the weighting or covariance matrix, and A and B are weighting variables to scale the different components of the objective function. According to Gribb (1996), these weighting variables should be equal to the inverse square of the mean measured value to account for unequal units and magnitudes:

$$A = \left[\frac{1}{N} \sum_{j=1}^N \tau_p(t_j) \right]^{-2}, \quad [35]$$

and

$$B = \left[\frac{1}{M} \sum_{i=1}^M h(t_i) \right]^{-2} \quad [36]$$

A single pressure head measurement in the dry region of the retention curve is critical in differentiating among the α and n pairs that have equivalent errors (Fig. 5A). As a result, simulations B1 and B2 include one pressure head measurement at $z = 1.5$ m bgs and $t = 0$ s to help resolve the values of both α and n . From Fig. 2, a value of -490 cm was assigned for the pressure head. Even though simulations B1 and B2 started from extreme regions of parameter space, they converged to almost identical, accurate predictions of α and n . The retention curves associated with the inverted parameters from simulation B1 (Fig. 5B) show a better match to the retention curve used in the forward model than those determined without a supporting pressure head measurement (Fig. 5A).

CONCLUSIONS

An analytical unsaturated flow model and an analytical BGPR ray-tracing model were used to evaluate the inversion of hydraulic parameters based on ZOP BGPR measurements made during infiltration. The models predicted a period of increasing travel time with infiltration time for sharp wetting fronts. A parameter estimation code was coupled with the forward models to invert the hydraulic parameters from BGPR observations with the objective of minimizing the difference between the modeled and measured first arriving BGPR travel times. It was shown that if the wetting front is sharp enough to produce a period of linearly increasing first arrival travel time with infiltration time, then the hydraulic conductivity behind the wetting front can be determined from the BGPR measurements alone. If the infiltration rate is too low to produce saturated conditions behind the wetting front, then an estimate of the effective saturation is needed to determine K_{sat} . The van Genuchten α and n parameters cannot be obtained uniquely from BGPR travel time data alone. However, the inclusion of a single pressure head measurement in the dry portion of the retention curve allows for unique inversion of both α and n . The method as presented in this paper only made use of travel time measurements collected at a single depth. However, the speed of profiling that is achievable with ZOP BGPR would also allow for repeated profiling during the course of an infiltration experiment to determine the vertical distribution of hydraulic parameters. Thus, this ability of BGPR to collect high-resolution water content profiles presents a possible advantage of BGPR for hydrologic parameter estimation.

The analysis presented in this paper was limited to a homogeneous synthetic, error-free example to demonstrate a proof-of-concept for using ZOP BGPR travel time measurements to obtain hydraulic properties. The concept directly couples a hydrologic and geophysical model for a multiphysics representation of the proposed field experiment. Commonly, geophysical data is indirectly incorporated through statistical means, where a

geophysical parameter is measured in the lab or field under differing hydrologic conditions and correlations are made with the parameter of interest (e.g., Hubbard et al., 2001). Geophysical field measurements are then conducted separate from hydrologic measurements and the new hydrologic variable is represented using Bayes theorem to update the prior probability density function of the original hydrologic variable. The method presented in this paper is a unique approach to incorporating BGPR data for hydrologic parameter estimation, and can be adapted to other types of geophysical measurements, for example, electrical resistivity tomography, thermalized neutron measurements, electromagnetic induction, or any other method that can obtain a representation of the water content during transient process in the vadose zone.

REFERENCES

- Archie, G.E. 1942. The electrical resistivity log as an aid to determining some reservoir characteristics. *Trans. AIME* 146:389–409.
- Binley, A., G. Cassiani, R. Middleton and P. Winship. 2002. Vadose zone flow model parameterisation using cross-borehole radar and resistivity imaging. *J. Hydrol. (Amsterdam)* 267:147–159.
- Brooks, R.H., and A.T. Corey. 1964. Hydraulic properties of porous media. *Hydrology Paper 3*, Colorado State University, Fort Collins.
- Davis, J.L., and A.P. Annan. 2002. Ground penetrating radar to measure soil water content. p. 446–463 *In* J.H. Dane and G.C. Topp (ed.) *Methods of soil analysis*. Part 4. SSSA, Madison, WI.
- de Lima, O.A.L., and S. Niwas. 2000. Estimation of hydraulic parameters of shaly sandstone aquifers from geoelectrical measurements. *J. Hydrol. (Amsterdam)* 235:12–26.
- Doherty, J. 2002. PEST: Model-independent parameter estimation v4. Watermark Numerical Computing.
- Ferré, P.A., D.L. Rudolph, and R.G. Kachanoski. 1996. Spatial averaging of water content by time domain reflectometry: Implications for twin rod probes with and without dielectric coatings. *Water Resour. Res.* 32:271–279.
- Ferré, P.A., J.H. Knight, D.L. Rudolph, and R.G. Kachanoski. 1998. The sample area of conventional and alternative time domain reflectometry Probes. *Water Resour. Res.* 34:2971–2979.
- Finsterle, S., and B. Faybishenko. 1999. Inverse modeling of a radial multistep outflow experiment for determining unsaturated hydraulic properties. *Adv. Water Resour.* 22:431–444.
- Gribb, M. 1996. Parameter estimation for determining hydraulic properties of a fine sand from transient flow measurements. *Water Resour. Res.* 32:1965–1974.
- Hopmans, J.W., and J. Simunek. 1999. Review of inverse estimation of soil hydraulic properties. p. 963–1008. *In* M.Th. van Genuchten et al. (ed.) *Proc. of the international workshop on characterization and measurement of the hydraulic properties of unsaturated porous media*. University of California, Riverside.
- Hopmans, J.W., J. Simunek, N. Romano, and W. Durner. 2002. Inverse Methods. p. 963–1008. *In* J.H. Dane and G.C. Topp (ed.) *Methods of soil analysis*. Part 4. SSSA, Madison, WI.
- Hubbard, S., Y. Rubin, and E. Majer. 1998. Estimation of hydrogeological parameters and their spatial correlation structure using geophysical methods. *IAHS Publ.* 250:503–512.
- Hubbard, S.S., J. Chen, J. Peterson, E.L. Majer, K.H. Williams, D.J. Swift, B. Mailloux, and Y. Rubin. 2001. Hydrogeological characterization of the South Oyster bacterial transport site using geophysical data. *Water Resour. Res.* 37:2431–2456.
- Inoue, M., J. Simunek, J.W. Hopmans, and V. Clausnitzer. 1998. In-situ estimation of soil hydraulic functions using a multistep soil-water extraction technique. *Water Resour. Res.* 34:1035–1050.
- Kirkham, D., and W.L. Powers. 1972. *Advanced soil physics*. John Wiley & Sons, New York.
- Klute, A.A. 1952. Numerical method for solving the flow equation for water in unsaturated materials. *Soil Sci.* 73:105–116.
- Lambot, S., M. Javaux, F. Hupert, and M. Vanclooster. 2002. A global multilevel coordinate search procedure for estimating the unsaturated soil hydraulic properties. *Water Resour. Res.* 38:1224.
- Parker, J.C., J.B. Kool, and M.Th. van Genuchten. 1985. Determining soil hydraulic properties from one-step outflow experiments by parameter estimation: II. Experimental Studies. *Soil Sci. Soc. Am. J.* 49:1354–1359.
- Perroux, K.M., and I. White. 1988. Designs for disk permeameters. *Soil Sci. Soc. Am. J.* 52:1205–1215.
- Philip, J.R. 1957a. The theory of infiltration: 1. The infiltration equation and its solution. *Soil Science* 83:345–357.
- Philip, J.R. 1957b. The theory of infiltration: 2. The profile at infinity. *Soil Sci.* 83:435–448.
- Philip, J.R. 1969. Theory of Infiltration. *Adv. Hydrosociences* 5:215–296.
- Richards, L.A. 1931. Capillary conduction of liquids through porous mediums. *Physics* 1:318–333.
- Rucker, D.F., and T.P.A. Ferré. 2003. Near-surface water content estimation with borehole ground penetrating radar using critically refracted waves. *Vadose Zone J.* 2:247–252.
- Rucker, D.F., and T.P.A. Ferré. 2004a. Automated water content reconstruction of zero-offset borehole ground penetrating radar data using simulated annealing. *J. Hydrology (Amsterdam)* (in review).
- Rucker, D.F., and T.P.A. Ferré. 2004b. Correcting water content measurement errors associated with critically refracted first arrivals on zero offset profiling borehole ground penetrating radar profiles. *Vadose Zone J.* 3:278–287.
- Rucker, D.F., and T.P.A. Ferré. 2004c. BGPR_Reconstruct: A MATLAB ray-tracing program for nonlinear inversion of first arrival travel time data from zero-offset borehole radar. *Comput. Geosci.* (in press).
- Sheriff, R.E., and L.P. Geldart. 1995. *Exploration seismology*. Cambridge University Press, Cambridge.
- Si, B.C., and R.G. Kachanoski. 2000. Estimating soil hydraulic properties during constant flux infiltration: Inverse procedures. *Soil Sci. Soc. Am. J.* 64:439–449.
- Simunek, J., and M.Th. van Genuchten. 1996. Estimating unsaturated soil hydraulic properties from tension disc infiltrometer data by numerical inversion. *Water Resour. Res.* 32:2683–2696.
- Toorman, A.F., P.J. Wierenga, and R.G. Hills. 1992. Parameter estimation of hydraulic properties from one-step outflow data. *Water Resour. Res.* 28:3021–3028.
- Topp, G.C., J.L. Davis, and A.P. Annan. 1980. Electromagnetic determination of soil water content: Measurements in coaxial transmission lines. *Water Resour. Res.* 16:574–582.
- van Genuchten, M.Th. 1980. A closed-form equation for predicting the hydraulic conductivity of unsaturated soils. *Soil Sci. Soc. Am. J.* 44:892–898.
- Vrugt, J.A., W. Bouten, and A.H. Weerts. 2001. Information content of data for identifying soil hydraulic parameters from outflow experiments. *J. Hydrol. (Amsterdam)* 65:19–27.
- Wang, W., S.P. Neuman, T.-M. Yao, and P.J. Wierenga. 2003. Simulation of large-scale field infiltration experiments using a hierarchy of models based on public, generic, and site data. *Vadose Zone J.* 2:297–312.
- Warrick, A.W. 1993. Inverse estimates of soil hydraulic properties with scaling: One dimensional infiltration. *Soil Sci. Soc. Am. J.* 57: 631–636.
- Warrick, A.W. 2003. *Soil water dynamics*. Oxford University Press, Oxford.
- Warrick, A.W., D.O. Lomen, and S.R. Yates. 1985. A generalized solution to infiltration. *Soil Sci. Soc. Am. J.* 49:34–38.
- Whisler, F.D., K.K. Watson, and S.J. Perrens. 1972. The numerical analysis of infiltration into heterogeneous porous media. *Soil Sci. Soc. Am. J.* 36:868–874.
- Yeh, T.-C., S. Liu, R.J. Glass, K. Baker, J.R. Brainard, D. Alumbaugh, and D.A. LaBrecque. 2002. A geostatistically based inverse model for electrical resistivity surveys and its application to vadose zone hydrology. *Water Resour. Res.* 38:14.1–14.13.